Electrophoresis of Composite Molecular Objects. 1. Relation between Friction, Charge, and Ionic Strength in Free Solution

Claude Desruisseaux,[†,‡] Didier Long,[§] Guy Drouin,[‡] and Gary W. Slater*[,†]

Department of Physics and Department of Biology, University of Ottawa, Ottawa, Ontario K1N 6N5, Canada, and Université de Paris XI, Laboratoire de Physique des Solides, bât. 510, 91405 Orsay Cedex, France

Received February 14, 2000; Revised Manuscript Received October 24, 2000

ABSTRACT: We present a study of the mobility of streptavidin end-labeled ssDNA fragments in free solution capillary electrophoresis. Our data show that the contribution of the uncharged streptavidin label to the net electrophoretic mobility of the complex depends on the buffer ionic strength because this frictional contribution is actually related to the persistence length of the ssDNA fragment. Therefore, the ionic strength of the buffer affects both the free-solution mobility of naked ssDNA and the effective slowing down (or "drag") due to the streptavidin label. We further show that our experimental results can be interpreted using recently published polyelectrolyte electrophoresis theories. Our results thus confirm that the so-called free-draining picture of local ssDNA electrophoretic friction and charge is not valid.

1. Introduction

Single-stranded DNA (ssDNA) is a polyelectrolyte whose electrophoretic mobility does not normally depend on its contour length.[1] This is why ssDNA separation cannot be obtained in free-solution electrophoresis. However, two methods to separate ssDNA using free-solution have recently been proposed. The first method requires uncharged labels[2] whereas the second one uses the electroosmotic flow (EOF).[3] Here, we examine the first method, called end-labeled free-solution electrophoresis (ELFSE), and the physics underlying ELFSE separations.[4,5] Our first theoretical paper about ELFSE[2] made predictions about the resolution of this new method using a very simple analytical model with empirical parameters that were rather ill-defined. The present article bridges the gap between the original ELFSE concept,[2] a new theoretical model of electrophoresis,[6−10] recent data,[5] and our new experimental results.

The size independence of the electrophoretic mobility of ssDNA in free solution is a consequence of the uniformity of these molecules and is a general feature of polyelectrolytes.[11] Labeling the ssDNA fragments with a different type of molecule, the key idea of ELFSE, makes the chain nonuniform and renders free-solution separation possible. In this article, we will limit ourselves to the case of the streptavidin-ssDNA complexes used by Heller et al.[4] and Ren et al.[5] We will consider that the residual charge of the streptavidin label is exactly zero in order to facilitate data analysis (our recent ELFSE results indicated that it has a very small charge).[5] We will also deliberately avoid discussing labels that can be deformed during electrophoresis since this leads to quite different situations.

The feasibility of ssDNA sequencing using ELFSE, first discussed in 1994,[2] was recently demonstrated by Ren et al.[5] In the original theoretical treatment of this problem, the limitations of ELFSE as a sequencing technique were estimated assuming the absence of electrostatic and hydrodynamic interactions between the ssDNA and the friction generating label and using a local model of free-flow electrophoresis. The traditional picture for describing the electrophoretic motion of a single ssDNA molecule has long been that the mobility is the ratio between an effective charge Q, proportional to the contour length of the fragment, and an electrophoretic friction coefficient, also proportional to the contour length. This free draining picture yields the well-known experimental result of a size-independent electrophoretic mobility for uniformly charged chains. However, this can lead to erroneous interpretations in more general situations where both nonelectric and electric forces are simultaneously applied or in the case of nonuniformly charged objects such as those studied here.[8,10] In light of the new theoretical approach for the electrophoretic migration of composite molecular objects developed by Long et al.,[6−10] the theory of ELFSE must be revisited.

This article is not intended to explain every aspect of the new theory. Instead, our aim here is to describe new experimental results that can be used to test this new theory. The concepts of hydrodynamic friction coefficients, ssDNA stiffness, and buffer ionic strength will be discussed, and we will show how they are intimately related. One cannot understand (or optimize) the ELFSE separation process without a better and more fundamental understanding of those key concepts.

The article is organized as follows. First, we develop a model to estimate the electrophoretic mobility of such complexes using the polyampholyte theory of ref 10. This section focuses on the four length scales involved in the problem: the streptavidin radius R_S, the Debye length λ_D of the solution, the contour length M (in bases) of the fragment, and the persistence length p of ssDNA. The last two lengths can also be combined to yield the radius-of-gyration $R_G(M)$ of the given ssDNA fragment. We then describe our experimental method and our data. The latter are analyzed in terms of our model, and

[†] Department of Physics, University of Ottawa.
[‡] Department of Biology, University of Ottawa.
[§] Université de Paris XI.
* To whom correspondence should be addressed. Phone (613) 562-5800, ext. 6775; Fax (613) 562-5190; E-mail gslater@science.uottawa.ca.

10.1021/ma0002702 CCC: $20.00
Published on Web 12/08/2000

conclusions regarding the theory and the limitations of ELFSE are discussed.

2. Theory

2.1. Electrophoretic Mobility of ssDNA. In this subsection, we briefly discuss the free-flow electrophoretic mobility μ_0 of naked ssDNA fragments. Several regimes may appear according to the ionic strength I of the solution, the molecular size M of the fragments, and the persistence length $p(I)$ of ssDNA. A more quantitative description of the mobility is beyond the scope of this paper and is actually a very complex problem.[11−14] Note that a similar discussion has been recently proposed by Hoagland et al.[15]

Consider a charged particle immersed in an electrolyte solution. Ions of the solution bearing an opposite charge are attracted by the particle, while ions with the same sign are repulsed. These interactions result in the building up of a charged layer around the particle, with the same total charge but opposite sign: this is the Debye layer of thickness λ_D. The Debye length λ_D (the screening length of electrostatic interactions) is a property of the electrolyte solution, and it varies as the inverse of the square root of the ionic strength I of the solution, $\lambda_D \sim 1/I^{1/2}$. The Debye layer is usually described by solving the so-called Poisson−Boltzmann equations. The Poisson equation relates the charge density in the solution to the local electric potential, and the Boltzmann equation relates the charge density to the electric potential by imposing that the density of charged particles follows the Boltzmann distribution; this is a mean-field picture. However, the structure of the Debye layer deserves some closer discussion, as emphasized by Manning in the case of, e.g., strongly charged rods.[16] Indeed, another length scale is of importance when considering charged objects in an electrolyte: the Bjerrum length l_B is the distance at which the electrostatic interaction energy between two electrons in the solution (which is then seen as a dielectric medium) is equal to the thermal energy k_BT. In water at room temperature, the Bjerrum length is $l_B \cong 7$ Å. When the charge density ρ along such a rod is weak, i.e., less than one electron charge per Bjerrum length ($\rho < \rho_B = e/l_B$), linearization of the Poisson−Boltzmann equations is possible, and one finds that the charge density of the counterions cloud is essentially a decreasing exponential of characteristic length λ_D. On the other hand, when the rod bears a charge density $\rho > e/l_B$, nonlinear effects become important. The Debye layer can be schematically divided into two parts: a first part very close to the rod, within a distance typically of a few angstroms, where the excess of counterions essentially cancels the density of charge in excess of one electron per Bjerrum length. Beyond this distance, the rod can be seen as bearing a charge density $\rho_B = e/l_B$, and linearization of the Poisson−Boltzmann equations is possible. One has then a smooth exponential decay of the charge density in the solution, corresponding to the reduced charge density $\rho_B = e/l_B$. This is the Manning condensation. For a review of these issues, see e.g. Barrat and Joanny.[17]

Let us consider ssDNA fragments. Such fragments bear the charge of one electron per base, i.e., one charge per contour length $b = 4.3$ Å, the ssDNA monomer size. Thus, Manning condensation is expected to occur and to reduce the apparent charge density of the ssDNA to $\rho = \rho_B$. In other words, beyond a few angstroms distance, ssDNA fragments can be considered as bearing one electron per Bjerrum length, and linearized Poisson−Boltzmann theory applies: beyond a molecularly thin sheet covering the ssDNA backbone, the chain is surrounded by a cloud of counterions essentially evenly distributed over a layer of thickness λ_D. The total charge density of this counterions cloud is $-\rho_B$.

As far as electrophoretic properties are concerned, ssDNA can be considered as a uniformly charged chain. In the limit of long fragments, as mentioned above, the mobility is independent of the size.[1,11] Indeed, for the usual case of uniform polyelectrolyte chains with radii of gyration larger than the Debye length ($R_G > \lambda_D$), the mobility results from a local balance at the scale of the Debye length between two effects: the electric force which acts directly on the chain and the friction due to the flow resulting from the action of the field on the counterions. Thus, the electrophoretic motion of the chain is slowed as compared to Stokes motion due to the presence of the counterions. The closer the counterions to the chain backbone, the stronger the effect. In a precise approach, one would have to solve the electrohydrodynamic equations with a no-slip condition on a shear layer, taking into account the distribution of charge given by the nonlinear Poisson−Boltzmann equations beyond the shear layer, following a model proposed by Schellman and Stigter,[14] which they solved numerically. However, the precise location of the shear layer, and the amount of condensed counterions it contains, is an adjustable parameter in Schellman and Stigter's model. Moreover, we do not pretend to propose a precise model for the electrophoretic motion but to discuss qualitatively the dependence of the mobility according to the various relevant parameters such as the salt concentration and the persistence length of ssDNA. In the qualitative picture that we propose, and following Manning,[11] we consider then that the effect on the chain's motion of Manning's condensed fraction amounts to canceling the direct action of the opposite charge on the backbone. The electrophoretic properties are then that of a backbone with a reduced effective charge, i.e., one electron per Bjerrum length, surrounded by the corresponding cloud of counterions that can be described within the linear Debye−Hückel theory. Contrary to the case of sedimentation, no collective effects on length scales larger than λ_D are present because the ensemble constituted by the chain and the surrounding counterions is neutral. Since the chain is uniform, all sections move at the same velocity in some kind of free fall. Therefore, the mobility of a ssDNA fragment is essentially that of a subfragment having a radius of gyration equal to the Debye length λ_D.

Let us now consider a few important cases that may occur, according to the relative value of the persistence length, the radius of gyration, and the Debye length.

2.1.1. R_G Smaller Than the Debye Length ($R_G < \lambda_D < p$). In this regime, one has a very short charged and rigid object, surrounded by noncondensed counterions. This in fact corresponds to the situation found with large Debye lengths and small charged spheres,[11] a historical problem studied by Henry.[13,17] However, the counterions can be considered as being far from the object (see Figure 1), and the friction of the electroosmotic flow they induce on the chain is small. The electrophoretic motion of the object is then essentially equivalent to a sedimentation motion, i.e., the motion under the action of a nonelectric force which would act only on the chain. The mobility is the charge of the chain

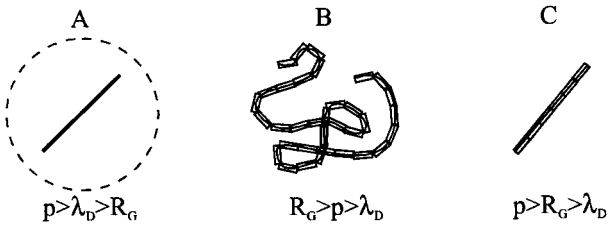

Figure 1. Schematic representation of a polyelectrolyte for different experimental conditions. The three different regimes shown here are (A) $p > \lambda_D > R_G$; (B) $R_G > p > \lambda_D$; (C) $p > R_G > \lambda_D$. In each case, the independent hydrodynamic blobs of size λ_D are shown.

divided by its hydrodynamic friction $\xi(M)$:

$$\mu_0(M) = \frac{Q(M)}{\xi(M)} \tag{1}$$

where $Q(M)$ is now the Manning effective charge of the chain $Q(M) = \rho_B Mb$. Note that we do not take relaxation effects into account here (i.e., the deformation of the counterions cloud; see ref 15 for a discussion on this point) since it is not necessary at this qualitative level. For a rod, the hydrodynamic friction coefficient is given by[18]

$$\xi(M) \approx \frac{3\pi\eta Mb}{\ln(M)} \tag{2}$$

(see Appendix A for more details). Equations 1 and 2 yield the mobility:

$$\mu_0(M) \approx \frac{Q(M)\ln(M)}{3\pi\eta Mb} \sim \ln(M) \tag{3}$$

The mobility is then expected to increase (slowly) with the molecular size M. This regime was not observed in our experiments.

2.1.2. R_G Larger Than the Debye Length ($R_G > \lambda_D$). As discussed above, the mobility of the polyelectrolyte (either a random coil ($R_G > p > \lambda_D$, Figure 1B) or a long rod ($p > R_G > \lambda_D$, Figure 1C)) is then equal to the mobility of subsections having a radius of gyration equal to the Debye length λ_D. The mobility of the subsection is that of a rigid rod of length λ_D and is given its Manning charge ($Q_D \sim \lambda_D$) divided by its friction coefficient (eq 2):

$$\mu_0 = \frac{Q_D \ln(\lambda_D/b)}{3\pi\eta\lambda_D} \sim \ln(\lambda_D/b) \tag{4}$$

Note that in this limit the mobility of rigid ($p > R_G$) and random coil ($R_G > p$) ssDNA fragments is the same since there is no hydrodynamic interaction between the "rigid" subsections of size λ_D.

2.1.3. Gaussian Chains. This short subsection describes a few additional theoretical elements that will be needed later when analyzing the ELFSE data in terms of a blob model of composite molecular objects subjected to electrophoretic and mechanical (drag) forces. The friction coefficient $\xi(M)$ of a random coil polymer chain is given by the Zimm limit,[19] i.e.

$$\xi(M) = 6\pi\eta R_H(M) \tag{5}$$

where η is the buffer viscosity and $R_H(M)$ is the hydrodynamic radius of the molecule.

For a Gaussian coil (in this paper, we will neglect the excluded-volume interactions because the DNA subchains (or blobs) that we will look at will be quite small,[20] as we will see later), the relationship between the radius of gyration R_G and the hydrodynamic radius is given by[19]

$$R_H(M) \cong \frac{2}{3}R_G(M) \tag{6}$$

with

$$R_G^2(M) = \frac{pL}{3} \tag{7}$$

Here, $L = Mb$ is the polymer contour length and b the monomer size ($b = 0.43$ nm for single-stranded DNA fragments).

However, when the ration L/p is not very large (this will be the case here), a better description of the dimensions of the wormlike polymer is provided by the Kratky−Porod equation

$$R_G^2(M) \approx \frac{pL}{3}\left[1 - 3\left(\frac{p}{L}\right) + 6\left(\frac{p}{L}\right)^2 - 6\left(\frac{p}{L}\right)^3\left(1 - e^{-L/p}\right)\right] \tag{8}$$

This equation leads to the right scaling laws for the radius of gyration R_G for low ($R_G \sim M$) and high ($R_G \sim M^{1/2}$, or eq 7) molecular weights.

Unfortunately, there is no simple and universal relation like eq 6 between R_H and R_G for the Kratky−Porod (or wormlike) chain. One expects eqs 5 and 6 to apply in the $L \gg p$ limit where the chain becomes truly Gaussian and eq 2 in the $L < p$ rigid-rod limit. In the latter case, eq 8 gives $R_G \cong L/12^{1/2}$, and eq 6 must be replaced by

$$\frac{R_H}{R_G} \cong \frac{2\sqrt{12}}{\ln(M)} \tag{9}$$

In most cases, we will be in the limit where eq 6 should be approximately valid. However, we will have to be careful since eq 9 gives a ratio larger than $^2/_3$ in the limit where it applies.

2.2. Mobility of the ssDNA−Streptavidin Complex. Let us now consider a Gaussian fragment to which a large neutral buoy, such as streptavidin, is attached (see Figure 2). This object is nonuniform for two reasons:

(a) The radius R_S of the streptavidin (≅2.5 nm) is larger than the diameter of the ssDNA backbone (≅1 nm). Moreover, R_S is not equal to the persistence length p of the ssDNA molecule (as will be discussed later, $p = p(I)$ is in fact a function of the ionic strength I).

(b) Unlike the ssDNA fragment, the buoy is essentially uncharged and has a negligible (or zero) electrophoretic mobility. At equilibrium, and for long ssDNA fragments, the buoy is immersed within the ssDNA Gaussian coil (Figure 2A). When an electric field E is applied, the ssDNA part of the complex tends to move according to its own electrophoretic mobility while the neutral buoy tends to slow down this motion. At low enough electric fields $E < E_0$, the equilibrium conformation of the complex (Figure 2A) is not perturbed, and the buoy remains within the ssDNA coil. For intermediate fields ($E_1 > E > E_0$), the coil and the buoy segregate because of the frictional effects, but the former retains its Gaussian conformation (Figure 2B).[9] Finally, at high fields $E > E_1$, the buoy and the ssDNA fragment assume

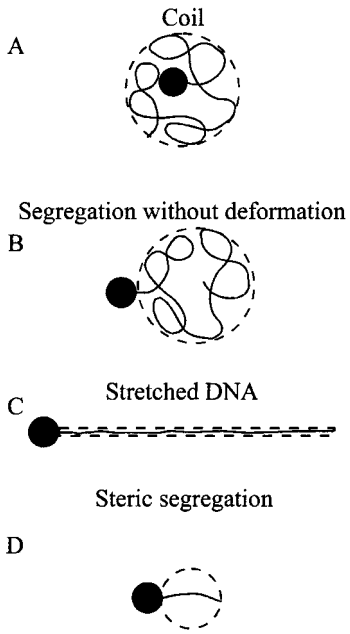

Figure 2. Schematic representation of the possible hydrodynamic conformations of the streptavidin−DNA complex. (A) The streptavidin and the ssDNA fragment form one hydrodynamic entity, and the streptavidin label is immersed within the ssDNA coil. (B) There is segregation of the ssDNA and streptavidin components, but the ssDNA remains almost undeformed. (C) Segregation and ssDNA stretching occur. (D) Steric segregation may be obtained for short enough ssDNA molecules when the persistence length is comparable to (or larger than) the size of the label.

a half-dumbell conformation with a fully stretched ssDNA section (Figure 2C).[9] The critical fields E_0 and E_1 will be discussed later. These situations correspond to following electrophoretic regimes:

2.2.1. Equilibrium Conformation. Let us consider the first regime, at low electric fields $E < E_0$, when the streptavidin is immersed within the ssDNA coil (Figure 2A). The electric field acts directly on the charged ssDNA fragment and pulls the complex in one direction. It also acts on the counterions surrounding the ssDNA fragment, which generate an electroosmotic flow that exerts additional friction on both the ssDNA fragment and the neutral buoy (since the latter is immersed within the coil). Recently, Long et al.[10] have described how one can calculate the electrophoretic mobility of a Gaussian polyampholyte made of monomers of equal sizes but of different individual electrophoretic mobilities (or different electric charges). Indeed, this situation is close to the one considered here, as the net electrophoretic mobility of the polyampholyte results from the friction of the global electroosmotic flow due to the counterions surrounding the different monomers. In fact, the electroosmotic flow of the counterions surrounding a given monomer also exerts a friction on all the other monomers. It has been shown that the electrophoretic mobility of such a polyampholyte is essentially the average of the mobility each monomer would have in a solution, independently from the others, provided the considered monomer length b_{eff} is larger than the Debye length of the solution.[10] Note that in the opposite case ($b < \lambda_D$) it is still possible to redefine the monomers (or blobs) by a coarse-graining procedure such that one recovers $b_{\text{eff}} > \lambda_D$.

The main point here is that our streptavidin−ssDNA complex can be seen as a polyampholyte by redefining the ssDNA monomers by a coarse-graining procedure. We define these new blob monomers as being made of α ssDNA bases, such that the hydrodynamic radius of these blobs is equal to the buoy radius R_S (which we suppose larger or equal to the Debye length). As a result, we obtain a "polyampholyte" made of $N + 1 = M/\alpha + 1$ coarse-grained monomers of radius R_S. The first monomer (the neutral buoy) has a zero electrophoretic mobility. The net mobility of the S-DNA complex is then given by the average of the individual mobilities of the b_{eff} blob monomers:[10]

$$\mu_{S-DNA}(M) = \frac{\sum_{i=1}^{N+1} \mu_i}{N+1} \approx \frac{\mu_0}{1 + \frac{\alpha}{M}} \tag{10}$$

where M is the molecular weight of the ssDNA fragment (in bases), and μ_0 is the electrophoretic mobility the new ssDNA monomers would have individually in a free-flow electrophoresis experiment. The mobility of the complex will then depend on the number (α) of ssDNA bases contained within a new blob monomer as well as on the mobility μ_0 of these ssDNA monomers. Note that the ratio μ_{S-DNA}/μ_0 thus depends on the ssDNA persistence length $p(I)$.

Let us emphasize that eq 10 is different from the result one would obtain using the free-draining model. According to the latter, the mobility of the complex would be the effective charge $Q \sim M$, divided by the sum of the friction coefficients of the DNA ($\xi \sim M$) and of the streptavidin ($\xi_S = 6\pi\eta R_S$). The mobility of the complex would then be given by

$$\mu_{S-DNA}(M) = \frac{\mu_0}{1 + \frac{\beta}{M}} \tag{11}$$

where $\beta = \xi_S/(\xi/M)$ would be the ratio between the hydrodynamic friction of the label and the "local electrophoretic friction" ξ/M of a single ssDNA monomer. Using the free draining picture, one thus obtains a similar form for the ratio μ_{S-DNA}/μ_0, the result originally obtained in ref 2. However, the ratio μ_{S-DNA}/μ_0 (or the constant β) would be independent of the ssDNA persistence length p or of the solution ionic strength I. Our results show a strong dependence and hence demonstrate that this free-draining picture of ELFSE is not valid.

2.2.2. Hydrodynamic Segregation. Consider the situation where the ssDNA coil and its buoy segregate (Figure 2B). This is a crossover regime between those described in sections 2.2.1 and 2.2.3. This situation has been considered by Long et al.[9] in the case of a diblock copolyelectrolyte. Because of the segregation between the buoy and the ssDNA chain, one can consider that the hydrodynamic friction of the complex is the sum of the hydrodynamic frictions of its components $\xi_{S-DNA} = \xi_{DNA} + \xi_S$. In an electrophoresis experiment, the ssDNA coil tends to move at its own electrophoretic mobility, while the buoy slows down this motion. Here, one can consider that the ssDNA pulls the buoy with a force $f = \xi_S \mu_{S-DNA} E$, while the buoy pulls the coil with an opposite force $-f = \xi_{DNA}(\mu_{S-DNA}E - \mu_0 E)$. As the ssDNA fragment has a globular conformation, the ssDNA hydrodynamic friction coefficient ξ_{DNA} is given by the Zimm coefficient

(eq 5). One then obtains

$$\mu_{S-DNA}(M) \approx \frac{\mu_0}{1 + \frac{R_S}{R_H(M)}} \qquad E_0 < E < E_1 \quad (12)$$

where $R_H \sim M^{1/2}$ for long enough ssDNA fragments.

2.2.3. Stretched ssDNA Fragments. For electric fields higher than a certain critical value E_1, the ssDNA fragment is fully extended (Figure 2C). This situation is analogous to the previous one, apart from the ssDNA fragment friction coefficient $\xi_{DNA}(M)$ which is now that of a longitudinally stretched oriented rod of length $L = Mb$:[18]

$$\xi_{DNA} \approx \frac{2\pi\eta Mb}{\ln(M) - {}^1/_2} \quad (13)$$

(see Appendix A). One then obtains

$$\mu_{S-DNA} \approx \frac{\mu_0}{1 + \frac{3R_S}{Mb}(\ln M - {}^1/_2)} \quad (14)$$

It is interesting to note that the molecular size dependence of the mobility is predicted to be (accidentally) almost the same in the high (eq 14) and low (eq 10) velocity regimes since the ($\ln M - {}^1/_2$) term is a weak function of M (it is a number of order unity).

Therefore, we may write

$$\mu_{S-DNA} \approx \frac{\mu_0}{1 + \frac{\alpha''}{M}} \qquad E > E_1 \quad (15)$$

where $\alpha'' = 3R_S(\ln M - {}^1/_2)/b$. However, the friction parameters α and α'' are quite different; for example, α does depend on the persistence length p of the ssDNA fragment (and hence on the ionic strength I), while α'' is independent of both p and I.

2.3. Ionic Strength. The Debye length is given by[21]

$$\lambda_D = \sqrt{\frac{\epsilon_b\epsilon_0 k_B T}{2e^2 I}} \quad (16)$$

where ϵ_b is the dielectric constant of the solvent, ϵ_0 is the permittivity of the vacuum, k_B is the Boltzmann constant, T is the absolute temperature, e is the charge of an electron, and I, the ionic strength of the buffer, is defined as

$$I = \frac{1}{2}\sum_k z_k^2 C_k \quad (17)$$

The sum is over the ionic species k, with z_k and C_k being the ion's valence and concentration (mol/L), respectively. The Debye length for ssDNA in an aqueous monovalent buffer is $\lambda_D \simeq 3.0$ Å$/I^{1/2}$ at 30 °C.[21] This value is usually quite small compared to the size of a ssDNA coil so that, for most practical cases, ssDNA is surrounded by a thin Debye layer and all ssDNA molecules have the same free mobility μ_0. In other words, we are in the case where $R_G > \lambda_D$ and the ssDNA mobility μ_0 is given by eq 4. The latter can be rewritten as

$$\mu_{DNA}(M) = \mu_0 \approx \frac{e}{3\pi\eta l_B}\ln\left(\sqrt{\frac{I_0}{I}}\right) \quad (18)$$

(where the parameter $I_0 = \epsilon_b\epsilon_0 k_B T/2e^2b^2$ has units of mol/L) since the charge of a section of length λ_D is then given by $Q = \lambda_D e/l_B$.

2.4. Relative ELFSE Friction Coefficient α. In principle, our theory allows us to determine the persistence length p of ssDNA using the measured values of the parameter α (see eq 10), which is predicted to be the molecular size of a ssDNA blob of hydrodynamic radius $R_H(\alpha \text{ bases}) = R_S$. As we will see, our α-blobs will contain between about 35 and 50 ssDNA monomers, while the ssDNA persistence length p typically corresponds to about 5−10 monomers.[22] These blobs thus contains a few (about 4−10) persistence lengths and must certainly be described as wormlike subchains. This means that one must use the Kratky−Porod eq 8 to calculate their radius of gyration R_G (indeed, using the Gaussian approximation eq 7 gave very poor fits; results not shown). Since our Kratky−Porod blobs are not close to the rigid-rod limit ($L \cong p$), we will use eq 6 as an approximate relationship between the blobs' radius of gyration R_G and their hydrodynamic radius R_H. Therefore, to a good approximation, we can write that the value of the parameter α should be directly related to the ssDNA persistence length p via the equation

$$R_S^2 = R_H^2(\alpha) \cong \left(\frac{2}{3}\right)^2 \frac{b\alpha p}{3}\left[1 - 3\left(\frac{p}{b\alpha}\right) + 6\left(\frac{p}{b\alpha}\right)^2 - 6\left(\frac{p}{b\alpha}\right)^3\left(1 - e^{-b\alpha/p}\right)\right] \quad (20)$$

where the radius of the streptavidin label is $R_S = 2.5$ nm. Note that for the streptavidin−ssDNA complex there is in fact no valid solution to this equation (for the persistence length p) when $\alpha < 30.21$. This critical value is obtained when the ssDNA backbone is so rigid that $p > R_S$; since the use of eq 6 becomes invalid in this limit anyway, we will have to be careful with the interpretation of data in this range.

2.5. Critical Electric Field E_0. The critical electric field E_0 necessary to achieve the hydrodynamic segregation between the ssDNA coil and the buoy corresponds to applying a counter-flow force $F_0 \geq k_B T/R_G(M)$ to the coil of radius of gyration $R_G(M)$, where $F_0 = 6\pi\eta R_H(M)\cdot(\mu_0 - \mu_{S-DNA})E$.[9] Using eq 10, the critical field E_0 can thus be written as

$$E_0 = \frac{k_B T}{4\pi\eta R_G^2(M)\mu_0}\frac{M + \alpha}{\alpha} \quad (21)$$

For a ssDNA fragment that is large enough to look like a random coil (i.e., $L \gg p$), we can use eq 7 to obtain

$$E_0 \approx \frac{3k_B T}{4\pi\eta b\mu_0}\frac{M + \alpha}{Mp\alpha} \quad (22)$$

Since $T = 30$ °C, $\eta \simeq 1$ cP, and $\mu_0 \cong 2 \times 10^{-4}$ cm^2/(V s) in our experiments, we get $E_0 \cong 0.116(M + \alpha)/M\alpha p$ [V/cm] (where p is in centimeters), which is much larger than the maximum electric field we could reach. When we use reasonable values such as $M = 300$, $p = 3$ nm,

and $\alpha = 50$, for instance, we get a very high value $E_0 \cong 9$ kV/cm. Therefore, under commonly used electrophoretic conditions, we expect to be in the segregation-free (and stretching-free) regime and α should be a function of the persistence length p of ssDNA (except perhaps at very low ionic strengths). Since the critical electric field E_1 would be even larger than E_0, it is completely irrelevant for this study.

2.6. Short Fragments and Steric Segregation. Even if the electric field is not high enough to obtain segregation (i.e., $E < E_0$), it is in principle possible to obtain some effective segregation when the persistence length is comparable to the size of the label and the ssDNA molecules are short (Figure 2D). If $p \geq R_S$, it may take a very long ssDNA fragment in order to completely "wrap" around the streptavidin label and make the latter look like a regular blob. Small ssDNA fragments (oligomers with a contour length $L < p$) will thus look "stretched", and they will be hydrodynamically segregated from the buoy. However, these rigid fragments will adopt a random orientation with respect to the electric field so that their friction coefficient will be given by[18]

$$\xi_{DNA} = \frac{3\pi\eta Mb}{\ln(M)} \tag{23}$$

This yields the mobility:

$$\mu_{S-DNA} \approx \frac{\mu_0}{1 + \frac{2R_S}{Mb}\ln M} \tag{24}$$

Note that even though these ssDNA fragments have the same conformation as electrically stretched ssDNA fragments ($E > E_1$), they do not have the same mobility because they are not oriented with the electric field. This very special case can only exist with small DNAs and at very low ioninc strengths since we need persistence lengths p to be comparable to R_S. We were not able to confirm the existence of this regime because, as we will discuss later, the necessary low ionic strengths destabilize the capillary coating that we used.

3. Materials and Methods

3.1. Electrophoresis Solutions. Solutions containing 3 M of urea (BDH), various concentrations (ionic strengths) of TAPS buffer (*N*-tris[hydroxymethyl]methyl-3-aminopropanesulfonic acid) (Sigma), and 0.04% (w/v) of poly(*N*,*N*-dimethylacrylamide) polymer (POP polymer; Applied Biosystems) were injected into the capillaries to perform the separation. The POP polymer, which is used solely to dynamically coat the capillary walls,[5] has a molecular weight of 10^6 g/mol, a polydispersity index PI = 3, and an entanglement concentration $c^* = 1.5\%$ w/v. This solution was buffered to pH = 8.4 (the pK_a of TAPS) with NaOH. A solution containing 1.0 mol/L of TAPS thus has an ionic strength of $I = 0.5$ mol/L.

3.2. ssDNA and S-DNA Samples. We used Pharmacia's 100 basepair ladder for our experiments. The two ends of these double-stranded DNA fragments are different, which allowed us to label only one of the strands. One end has a 5′ TCGG 3′ overhang whereas the other end has a 5′ CCGA 3′ overhang. The first step of the labeling procedure consisted in blocking the GG site of the first strand by adding deoxycytosine. We mixed 5 μL (5 μg) of 100 bp ladder, 5 μL of 5 × Amplitaq FS buffer (Applied Biosystems), 5 μL of dCTP (5 pmol/μL), 0.5 μL of Amplitaq FS, and 9.5 μL of dH_2O, and we allowed the filling reaction to proceed at 60 °C for 20 min. Unincorporated nucleotides were then removed using Centrisep columns (Princeton Separations). In the second step, we mixed the modified 100 bp ladder (17 μL) obtained in step one with 8 μL of 5HAmplitaq buffer, 4.5 μL of biotin-dUTP (148.5 pm), 2 μL of Cytosine Big Dye Terminator (Applied Biosystems) (21.5 pmol), 0.5 μL of Amplitaq FS, and 8 μL of dH_2O (for a total volume of 40 μL), and we allowed the reaction to proceed at 60 °C for 20 min. Centrisep columns were then used to remove the unincorporated nucleotides.

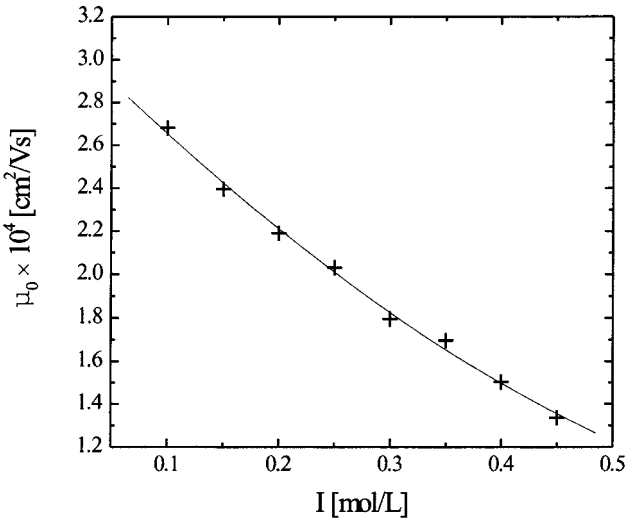

Figure 3. Free-solution ssDNA mobility μ_0 vs ionic strength I. The solid line is the second-order polynomial fit $\mu_0(I) = (3.16 - 5.32I + 2.91I^2) \times 10^{-4}$ cm^2/(V s).

The solution thus obtained was diluted 10 times with distilled water. The final DNA samples were produced by mixing 3 μL of this dilute solution with 10 μL of formamide and 6 μL of dH_2O. The streptavidin-labeled DNA (S-DNA) samples were obtained by adding an appropriate quantity of fractionated streptavidin to this solution[5] and heating at 65 °C for 5 min to separate the two strands. These denatured samples were subsequently kept on ice until they were used.

3.3. Electrophoresis Conditions. The running temperature (30 °C) was controlled through the thermostatic plate of the ABI PRISM 310 genetic analyzer capillary electrophoresis instrument. Experiments were performed on 45 cm long capillaries, and the applied voltage was 15 kV ($E = 33$ V/cm). Sample injection was performed at 15 kV for 5 s. The distance between the injection end of the capillary and the detector was 34 cm.

4. Results

4.1. ssDNA Free Mobility and Debye Length. To analyze the S-DNA mobility data using our theory, we need the free solution electrophoretic mobility μ_0 of naked ssDNA fragments. Figure 3 shows a plot μ_0 vs the ionic strength I of our TAPS buffer solutions (in mol/L). Unsurprisingly, μ_0 decreases smoothly when I increases. The curve was fitted using the empirical relation $\mu_0 = (3.16 - 5.32I + 2.91I^2) \times 10^{-4}$ cm^2/(V s) since it provided a decent fit over this range of ionic strengths. We did not observe any ssDNA separation in our experiments, even at low ionic strength, showing that we remained in the $\lambda_D < R_G(M)$ regime for all molecular sizes M used here. Figure 4 replots these data as μ_0 vs $\ln(1/I^{1/2})$, as suggested by eq 18. We do observe a reasonably linear behavior for $\ln(1/I^{1/2}) \lesssim 1.2$. Beyond that point (i.e., for ionic strengths $I < 0.09$ mol/L), the mobilities were anomalously low. We discovered that the main reason for these low mobilities was actually the fact that the pDMA dynamic coating of the capillary walls was unstable and unreliable in this limit (the EOF increases with time during the experiments at such low

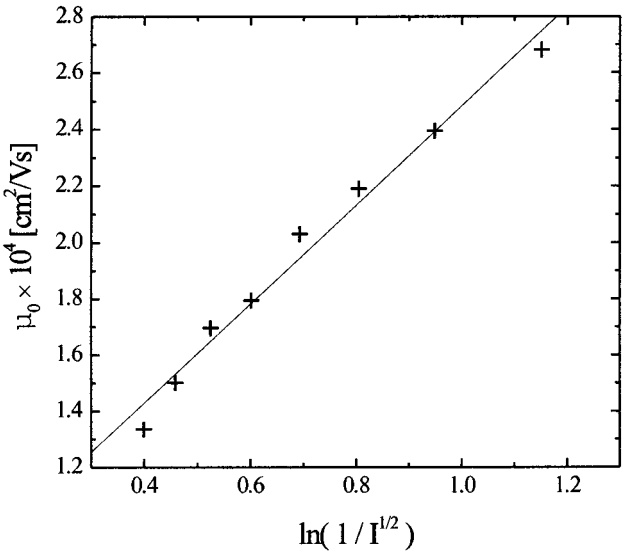

Figure 4. Free-solution ssDNA mobility μ_0 vs $\ln(I^{-1/2})$. The solid line corresponds to the linear fit $\mu_0 = (1.513 \times 10^{-4}) \times \ln[(3.098/I)^{1/2}]$ cm^2/(V s).

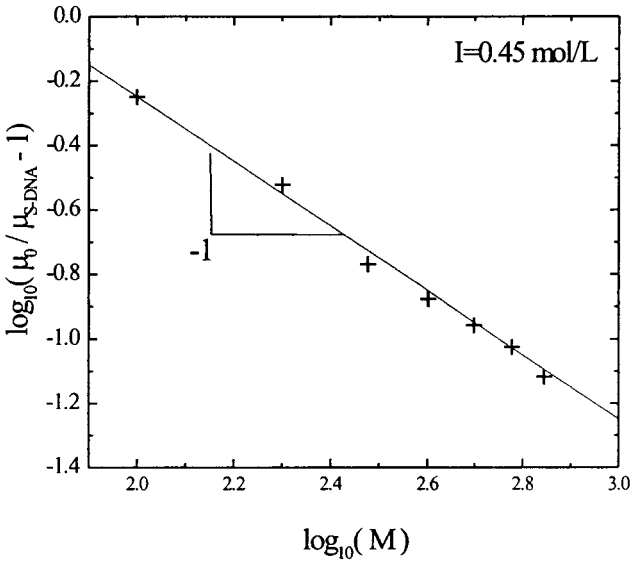

Figure 5. A log−log plot of $\mu_0/\mu_{S-DNA} - 1$ vs ssDNA size M (in bases) for a high salt content buffer solution ($I = 0.45$ mol/L).

ionic strengths, which reduces the measured mobilities). Therefore, we could not use lower ionic strengths (as a consequence, we could not explore the regime described in section 2.6). The linear fit gives $\mu_0 = 1.513 \times 10^{-4}$ $\ln[(3.098/I)^{1/2}]$ cm^2/(V s), which corresponds to $I_0 = 3.098$ mol/L and $e/(3\pi\eta l_B) = 1.513 \times 10^{-4}$ cm^2/(V s) (see eq 18). It is possible to estimate the monomer size using this value of I_0 and the fact that our definition of I_0 implies $b = (\epsilon_b \epsilon_0 k_B T/2e^2 I_0)^{1/2}$: we get $b = 0.18$ nm, consistent with the actual value of $b = 0.43$ nm. It is also possible to estimate l_B from the prefactor: we obtain $l_B \cong 11$ Å, in fair agreement with the value $l_B = 7$ Å.

4.2. Measuring the Value of α. In the limit where the two parts of the S-DNA molecule do not segregate, eq 10 predicts that $\mu_0/\mu_{S-DNA} - 1 = \alpha/M$. Figure 5 shows a log−log plot of $\mu_0/\mu_{S-DNA} - 1$ as a function of molecular size M for $I = 0.45$ mol/L. In agreement with the model, we obtain a slope of −1, and the fit gives the value $\alpha = 57.2$ for the relative friction coefficient of the buoy. This is much smaller than the value of $\alpha'' \approx 91$ (using $M =$ 300) predicted for stretched S-DNA molecules. As discussed previously, we are quite far from the stretching limit since our field ($E = 333$V/cm) is much smaller than the critical field $E_0 \cong 9$ kV/cm predicted for ssDNA/streptavidin segregation to happen. The method presented here was used to obtain the value α for all our data sets.

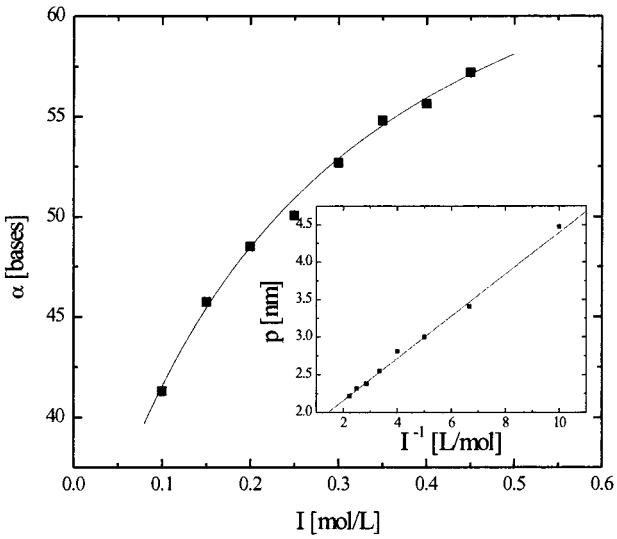

Figure 6. Relative friction coefficient of the streptavidin label (α) vs the ionic strength I of the buffer [in mol/L]. Inset: plot of p (in nm), calculated from the data of the main part of Figure 6, as a function of $1/I$. The linear fit gives $p = (1.6 + 0.28/I)$ nm.

4.3. Buoy Relative Friction Coefficient α and the ssDNA Persistence Length *p*. Figure 6 shows a plot of α as a function of the ionic strength I (α was found using eq 10 to fit the data, as shown in Figure 5). We see that α increases smoothly when we increase the concentration of salt in the buffer solution. This is in agreement with the fact that the persistence length of ssDNA decreases with increasing ionic strength. In other words, we need more ssDNA bases to form a blob that has a hydrodynamic radius $R_H = R_S$ when we increase the flexibility of ssDNA (or decrease the ionic strength). Let us stress that this dependence of α on the ionic strength invalidates the free-draining picture, according to a discussion above.

From the value of α, it is possible to estimate the persistence length p of ssDNA using eq 20 and the standard value of $b = 0.43$ nm; the results are shown in the inset of Figure 6. A linear behavior is obtained when p is plotted vs $1/I$, showing that the relation $p = p_0 + A/I$ is appropriate. Here, p_0 is the intrinsic or elastic persistence length of ssDNA (i.e., the persistence length it would have if it were an uncharged molecule). This relationship is in agreement with the prediction of Ha and Thirumalai.[23] The intrinsic persistence length of ssDNA, $p_0 = 1.6$ nm, is slightly higher than the one estimated by Tinland et al.,[22] 0.8 nm < p_0 < 1.3 nm, using diffusion measurements. In fact, our fit $p = (1.6 + 0.28/I)$ nm gives values that are higher than the ones estimated by Tinland over the whole range of ionic strengths. This might be due in part to the fact that we have neglected excluded-volume effects and assumed that the relation between the hydrodynamic radius and the radius of gyration is always $R_H/R_G \simeq 2/3$; in addition, we used a different buffer. The solid line in the main part of Figure 6 gives the value of α obtained from eq 10 when using our $p(I)$ relationship. The maximum

value of α thus predicted is $\alpha = 71.4$, which corresponds to $I \rightarrow \infty$ and $p = p_0$, while the minimum value $\alpha = 30.21$ (obtained when $p(I) = R_S$) is predicted to occur at $I = 0.0006$ mol/L. The combination of the two curves in Figure 6 indicates that our α-blobs contain between about 11 (for the highest ionic strength) and 4 (for the lowest ionic strength used here) ssDNA persistence lengths. In these cases, neglecting the excluded-volume interactions and using eq 6 to relate the blobs' hydrodynamic radius to their radius of gyration are reasonable approximations.

5. Discussion

In this article, we showed that the ionic strength plays an important role during ELFSE because it affects several key parameters. Usually, ssDNA is considered to be a random coil on length scales larger than its persistence length p. However, the situation is far more complex when one tries to understand the electrophoretic properties of ssDNA or of hybrid molecules such as our streptavidin−ssDNA complexes. To fully understand the physics underlying ELFSE, for instance, one must actually consider four different length scales: the radius of gyration of the ssDNA molecule $R_G(M)$, its persistence length p, the Debye length λ_D, and the size of the globular label R_S. Our analysis showed that although a ssDNA coil can look globally flexible, its microscopic rigidity is an important element, especially when p and R_S are comparable.

In our experiments, we observe that the free mobility of ssDNA, μ_0, decreases with increasing ionic strength like $\mu_0 \propto \ln(1/I^{1/2})$ (eq 18) when $I > 0.1$ mol/L (Figure 4). Below this ionic strength, the residual EOF could not be controlled efficiently by the pDMA dynamic coating, and we could not trust the data.

It was shown that the addition of a rigid globular buoy at one end of ssDNA fragments makes their free-solution electrophoretic separation possible.[4] The first theoretical model of ELFSE made the assumption that there was no hydrodynamic interaction between the ssDNA and streptavidin components.[2] We showed that this assumption is only valid for unrealistically high electric fields (note, however, that longer ssDNA molecules and larger labels could easily satisfy this condition; see eqs 21 and 22). Our new theoretical approach describes the existence of three distinct regimes.

At "low" electric field, the ssDNA−streptavidin complex can be considered as one hydrodynamic unit, and the mobility is given by $\mu = \mu_0/(1 + \alpha/M)$, where α is closely related to the persistence length of ssDNA and the radius of the label. In fact, α is the molecular size of a ssDNA blob having the same friction coefficient as the label ($R_H(\alpha) = R_S$). Since the number of ssDNA bases in such a blob (α) decreases with increasing persistence lengths (p), there is a strong correlation between the observed value of α and the ionic strength I of the running buffer. From our values of $\alpha(I)$, we were able to estimate the persistence length $p(I)$ of the ssDNA fragments. Interestingly, measuring the electrophoretic mobility of end-labeled ssDNA provides an estimate of the persistence length of ssDNA (more precisely, the behavior of the persistence length as a function of the ionic strength). However, streptavidin may not be the optimal label for this purpose because it is not very large compared to p; this limits our ability at determining p via the Kratky−Porod equation. Nevertheless, our estimated persistence lengths are in good agreement with the predicted theoretical form $p = p_0 + A/I$.[23] Our results indicate that $p \simeq (1.60 + 0.28/I)$ nm. The value of our intrinsic persistence length $p_0 = 1.60$ nm is comparable to the value obtained using a method based on the measurement of diffusion coefficients,[22] although our p's are systematically higher than those of Tinland.[22] However, our results remain compatible with those of Tinland given the many approximations involved in deriving the persistence length.

In the second hydrodynamic regime, the higher electric fields induce the segregation of the complex. In that limit, however, the field is not yet high enough to stretch ssDNA, and the deformation of the ssDNA strand can be neglected. The total friction coefficient ξ_{S-DNA} is simply the sum of the individual component ξ_S and ξ_{DNA}, and the net mobility is given by $\mu = \mu_0/(1 + R_S/R_H(M))$. We were unable to observe this regime since the required electric field intensities are, for small ssDNA fragments, much higher than what can be achieved with commercial capillary electrophoresis instruments. In principle, this regime can also be observed at low fields $E < E_0$ when the persistence length is not much smaller than the radius of gyration R_G. We call this situation "steric segregation" since the segregation between the streptavidin and the ssDNA fragment is not due, in this case, to the drag forces. Unfortunately, we were not able to observe this effect.

The last regime is characterized by ssDNA stretching. The mobility equation is somewhat similar to that in the low-field regime, but with $\alpha \rightarrow \alpha'' = 3R_S(\ln M - {}^1/_2)/b$ (this gives, e.g., $\alpha'' \simeq 91$ for $M = 300$). These larger value of α could increase the quality of the separation. Moreover, there is a major benefit in using very high fields when we consider the effect of diffusion. The diffusion coefficient at low field is given by the Stokes−Einstein relation $D_M = k_BT/(6\pi\eta R_H(M))$. As far as hydrodynamics is concerned, a S-DNA molecule containing M bases is roughly equivalent to a DNA molecule with $M + \alpha$ bases. Since in general we have $M \gg \alpha > p$, we expect the scaling $D_M \sim 1/M^{1/2}$. In the opposite limit where DNA is stretched, one should have $D_M \sim 1/M$ and, consequently, much sharper bands. Clearly, the optimal ELFSE strategy remains to be established.

In conclusion, our new ELFSE theory can explain the experimental data reported in this article. It is worth mentioning that these results could not be accounted for using the free-draining picture. Therefore, the concept of free-draining does not seem to be relevant in electrophoresis, a point recently stressed by Long et al.[8] Electrophoresis of composite molecular objects, such as our S-DNA molecules, represents a fundamental test of our current understanding of electrophoretic phenomena. Another test would be to check whether the diffusion coefficient D of naked DNA molecules remains proportional to $1/M^{1/2}$ (the Zimm prediction[19] for a hydrodynamically permeable coil) during electrophoresis instead of the $1/M$ scaling predicted by a simple free-draining picture. This is currently under investigation in our group. In the next two parts of this series, we will examine the electrophoresis of S-DNA molecules in gels and dilute polymer solutions.

Acknowledgment. This work was supported by Research Grants of the Natural Science and Engineering Research Council (NSERC) of Canada to G.W.S. and G.D. and by a scholarship of the University of Ottawa awarded to C.D. The authors also thank Applied Bio-

systems for the donation of the Prism 310 capillary system and Dr. Hongji Ren for help during this project.

Appendix A

The friction coefficient of a cylinder of length L and of radius r is dependent upon its orientation vs its velocity, as discussed in Berg.[20] When the cylinder is oriented with the field direction (or the drag force), the friction coefficient is given by

$$\xi_{\parallel} = \frac{2\pi\eta L}{\ln \frac{L}{r} - \frac{1}{2}} \tag{A1}$$

When the orientation of the cylinder is perpendicular to the field direction, however, we have

$$\xi_{\perp} = \frac{4\pi\eta L}{\ln \frac{L}{r} + \frac{1}{2}} \tag{A2}$$

In the more general case where the cylinder is moving at random we have

$$\xi = \frac{3\pi\eta L}{\ln \frac{L}{r}} \tag{A3}$$

To apply these results to ssDNA, we must use the relations $L = Mb$ and $r \cong b$. We used the expression for the random orientation (eq A3) to derive eqs 3, 4, and 23 and the expression for an oriented cylinder (eq A1) to obtain eq 14.

References and Notes

(1) Olivera, B. M.; Baine, P.; Davidson, N. *Biopolymers* **1964**, *2*, 245.
(2) Mayer, P.; Slater, G. W.; Drouin, G. *Anal. Chem.* **1994**, *66*, 1777.
(3) Iki, N.; Kim, Y.; Yeung, E. S. *Anal. Chem.* **1996**, *68*, 4321.
(4) Heller, C.; Slater, G. W.; Mayer, P.; Dovichi, N. J.; Pinto, D.; Viovy, J. L.; Drouin, G. *J. Chromatogr. A* **1998**, *806*, 113.
(5) Ren, H.; Karger, A. E.; Oaks, F.; Menchen, S.; Slater, G. W.; Drouin, G. *Electrophoresis* **1999**, *20*, 2501.
(6) Long, D.; Viovy, J. L.; Ajdari, A. *Phys. Rev. Lett.* **1996**, *76*, 3858.
(7) Long, D.; Viovy, J. L.; Ajdari, A. *J. Phys.: Condens. Matter* **1996**, *8*, 9471.
(8) Long, D.; Viovy, J. L.; Ajdari, A. *Biopolymers* **1996**, *39*, 755.
(9) Long, D.; Ajdari, A. *Electrophoresis* **1996**, *17*, 1161.
(10) Long, D.; Dobrynin, A. V.; Rubinstein, M.; Ajdari, A. *J. Chem. Phys.* **1998**, *108*, 1234.
(11) Manning, G. S. *J. Phys. Chem.* **1981**, *85*, 1506.
(12) Muthukumar, M. *Electrophoresis* **1996**, *17*, 1167.
(13) Henry, D. C. *Proc. R. Soc. London, Ser. A* **1931**, *133*, 106.
(14) Schellman, J. A.; Stigter, D. *Biopolymers* **1977**, *16*, 1415.
(15) Hoagland, D. A.; Arvanitidou, E.; Welch, C. *Macromolecules* **1999**, *32*, 6180.
(16) Manning, G. S. *J. Chem. Phys.* **1969**, *51*, 924.
(17) Barrat, J. L.; Joanny, J. F. *Adv. Chem. Phys.* **1996**, *94*, 1.
(18) Berg, H. C. *Random Walks in Biology*, Princeton University Press: Princeton, 1993.
(19) des Cloizeaux, J.; Jannink, G. *Polymers in Solution: Their Modelling and Structure*; Oxford Science Publishers: New York, 1990.
(20) Viovy, J. L.; Heller, C.; Principles of Sized-Based Separations in Polymer Solutions. In *Capillary Electrophoresis in Analytical Biotechnology*; Righetti, P. G., Ed.; CRC Press: Boca Raton, FL, 1996.
(21) Israelachvili, J. *Intermolecular & Surface Forces*; Academic Press: San Diego, 1992.
(22) Tinland, B.; Pluen, A.; Sturm, J.; Weill, G. *Macromolecules* **1997**, *30*, 5763.
(23) Ha, B.-Y.; Thirumalai, D. *J. Chem. Phys.* **1999**, *110*, 7533.

MA0002702